Driver Arrival Sensing for Smart Car using WiFi Fine Time Measurements

Xiaolu Zeng*, Beibei Wang*† and K. J. Ray Liu*†
* University of Maryland, College Park, MD, 20740, USA.
† Origin Wireless Inc., Greenbelt, MD, 20770, USA.
E-mail: (xlzeng09, bebewang, kjrliu)@umd.edu.

***Abstract*—Driver arrival sensing which enables the car to detect an approaching driver has been playing an important role in the evolving smart car system. This paper presents a driver arrival sensing scheme based on the fine time measurement (FTM) released in the IEEE 802.11mc protocol. We observe that when the initiating station (ISTA, such as a mobile phone or WiFi client) keeps moving towards the response station (RSTA, usually a WiFi access-point (AP)), there exists a knee point of the WiFi-FTM range estimation after which the variation of the WiFi-FTM range estimations follows a stable trend regardless of the environment. Inspired by such an observation, we propose a joint knee point detection and driver arrival time estimation algorithm based on the trend of WiFi-FTM range estimations. Given the arrival time, the car (RSTA) can determine the right time to start the service requested by the driver. We implement the proposed method using commercial 802.11mc WiFi chipsets and conduct extensive experiments in different parking lots with different testers. The results show that the scheme can achieve $\geq 92.5\%$ accuracy with $\leq$ 1s arrival time estimation error.**

I. Introduction

With the proliferation of WiFi devices in the past several decades [1]–[4], many WiFi-based applications for smart car systems [5], [6] such as activity recognition [7], driver authentication [8] and Advanced Driver Assistance Systems (ADAS) [9]–[11] have emerged. While these applications are mainly for in-car use, there has not been many out-car applications such as driver arrival sensing that needs to be further explored.

Driver arrival sensing is often used in remote control including locking/unlocking the door, opening/closing the window/convertible tops and remote ignition key [12], [13]. While these applications focus more on the driver's presence sensing, there are many other applications which need to estimate the accurate arrival time of the driver (AToD). For example, a car needs to sense the AToD so that the air conditioner (AC) system can be turned on at a right time. Turning on the AC too early will cause extra energy consumption while turning on the AC too late may lead to an uncomfortable temperature when the driver arrives. In the future, the car system may consist of many service systems such as driver identification [8] to make it more intelligent. As a result, a smart car needs to sense the AToD so that it can manage multiple services properly such as starting a time-consuming service (e.g., driver identification) earlier while responding to a time-saving service (e.g., door close/open) later on. On the other hand, the current driver sensing system mainly applies a digital code matching and rolling scheme by wireless transponders, which has a serious security issue [14], [15]. As a result, security needs to be enhanced in the AToD sensing system as well.

To address the aforementioned challenges, this paper proposes an AToD sensing algorithm by leveraging the WiFi-FTM protocol introduced in IEEE 802.11mc [16], [17]. There are two main advantages by using WiFi than the traditional low-power transponders [12]. First, the larger coverage of WiFi devices enables an earlier detection of the AToD. Second, WiFi provides more secure encryptions such as Wired Equivalent Privacy (WEP) and Wi-Fi Protected Access (WPA) [18] than the present digital code identification and rolling systems [12]. In addition, the WifiRttScan app [19] release by Google in 2019 to measure the distance to nearby FTM-capable Wi-Fi access points (APs) makes the WiFi-FTM more available.

In this paper, we first evaluate the accuracy of the WiFi-FTM range estimations in the practical parking lots by using the commercial 802.11mc WiFi chipsets. We then show that there always exists a **knee point** after which the WiFi-FTM range estimations show a stable trend when the ISTA (driver/client) keeps moving towards the RSTA (fixed on a car). Based on such an observation, a novel algorithm is proposed to detect the knee point and estimate the AToD. Experiment results show that the proposed system can achieve $\geq 92.5\%$ accuracy with $\leq$ 1s error of the AToD estimation.

The rest of the paper is organized as follows. In Section II, we introduce the WiFi-FTM range estimation protocol followed by the knee point analysis. Section III elaborates on the knee point detection and AToD estimation algorithms. Experiment results are given in Section IV while Section V concludes this paper.

II. Distance Estimation Based on WiFi-FTM

A. Basics of WiFi-FTM

WiFi-FTM was released in IEEE 802.11mc [16], [17] to enable the range estimations between two WiFi cards by using the round trip time (RTT). As shown in Fig. 2, N FTMs in a single burst can be averaged to get a more accurate RTT estimations. The distance estimation $R_{\text{IS}}(k)$ at burst k between the ISTA and RSTA is given by

$$R_{\text{IS}}(k) = \frac{1}{2N}\sum_{n=1}^{N}[(t_4(k,n)-t_1(k,n))-(t_3(k,n)-t_2(k,n))]\cdot c \quad (1)$$

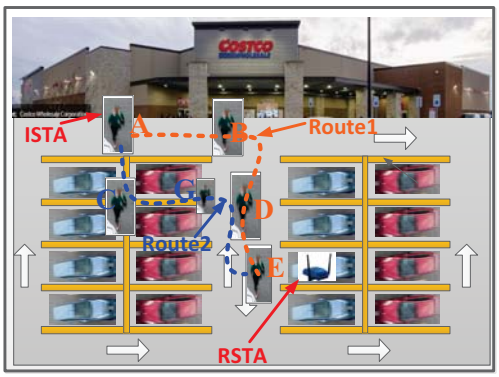

Fig. 1: Illustration of the system in a parking lot.

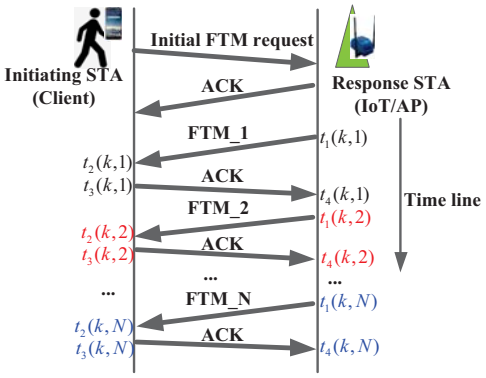

Fig. 2: Overview of FTM protocol.

where $c = 3 \cdot 10^8$m/s is the light speed. $t_1(k,n)$ and $t_4(k,n)$ denotes the departure and arrival time measured by the RSTA at burst k, pulse n. Similarly, $t_2(k,n)$ and $t_3(k,n)$ are the arrival and departure time recorded by the ISTA. Generally, $t_1(k,n)$ and $t_4(k,n)$ are sent back to ISTA for range estimations between the ISTA and RSTA. Note that the exchange of the FTMs and its acknowledgment frame (ACK) is usually finished within a very short period. Hence, the clock of the two stations do not drift significantly [20].

However, impacted by the multipath propagation and blockage in non-line-of-sight (NLOS) scenarios, the range estimation provided by (1) may not be accurate [16], [17]. An example is shown in Fig.1, where a user equipped with an ISTA is walking towards his car equipped with an RSTA. The user may approach the car along Route 1 (A→ B→D→E) or Route 2 (A→ C→G→D→E) or other routes. Taking Route 1 as an example, at the starting point 'A', the WiFi-FTM-based distance estimations are inaccurate due to NLOS of point A. However, as the user gets closer to the car, e.g., passing point 'B' (or point 'G' in Route 2), the LOS signal starts to dominate and the WiFi-FTM-based distance estimations become more accurate. It is expected that the distance estimations when the user approaches his car should exhibit a knee-point after which distance estimation becomes reliable.

B. WiFi-FTM Range Measurement

To verify the existence of the knee point in distance estimation, we conduct multiple experiments with settings as follows.

Hardware. We implement the WiFi-FTM using commercial 802.11mc WiFi chipsets as shown in Fig. 3. One WiFi chipset is integrated with the Intel Galileo control board to work as an RSTA which is fixed on top of a car during the test. Another WiFi chipset is installed on a Intel Apollo board to work as an ISTA. To build a mobile client, the ISTA is put in a box (named as TestBox) and carried by a tester in the test . The ISTA board runs Linux OS and receives instructions from a Surface Pro through an Ethernet cable. The Surface Pro works as an GUI through which we can control the ISTA such as sending/stopping request and get real time WiFi-FTM range estimations from the ISTA board.

Data Collection. In the experiment, the RSTA is fixed on top of a car in the parking lot and a tester holds the TestBox while moving towards the car from different directions and initial distances. Note that the initial distance means the distance between the ISTA and RSTA when the tester starts to move. Once the tester arrives at the car, he/she records the WiFi-FTM range estimation showing on the Surface Pro GUI manually as the ground truth of the arrival time T_{AM}. Different testers are invited to walk at different speeds. Extensive experiments have been conducted in different parking lots and garages on weekdays where the test car is surrounded by different cars during the data collection.

C. Analysis of Range Estimation

Fig. 4 shows the distance measurements with different initial distances and different directions, i.e., different routes $\mathbf{R}_1, \mathbf{R}_2, \cdots, \mathbf{R}_n$ in Fig. 3. To test the impact of the moving speed of the ISTA, Fig. 5 and Fig. 6 further show the results when a tester is running (about 3m/s) and walking slowly (about 1m/s) to the car. From Figs. 4 - 6, we can get the following observation.

The range estimations variate irregularly at the beginning and show a stationary trend passing a Knee Point. As shown in Figs. 4-6, we denote the moment when the tester gets to the car as **Arrival Time** T_{AM} which is labeled every time manually. At the beginning, the distance measurement changes randomly versus the walking time due to the random errors brought by the serious multipaths. As the ISTA keeps moving close to the RSTA, the distance measurements begin to decay linearly w.r.t. walking time. For example in Fig. 4-6, if we align the distance measurements according to the T_{AM}, the decaying trend is very consistent near T_{AM}. If we can detect such a knee point and estimate the accurate distance between the ISTA and RSTA as early as possible, the RSTA can predict the arrival time of the ISTA and response to the request from the ISTA properly. Next, we introduce a novel knee point detection and driver arrival time estimation method based on the aforementioned observations.

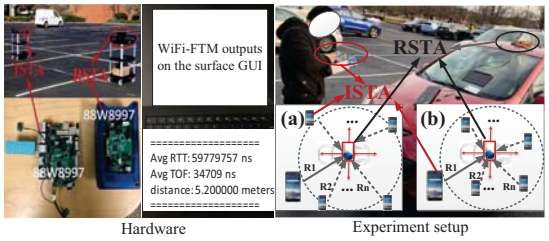

Fig. 3: Hardware and experiment setup. (a) The same initial distance. (b) Different initial distances.

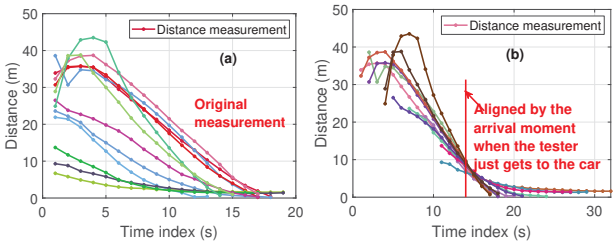

Fig. 4: Distance measurements when ISTA starts to approach the RSTA from different directions and initial distances.

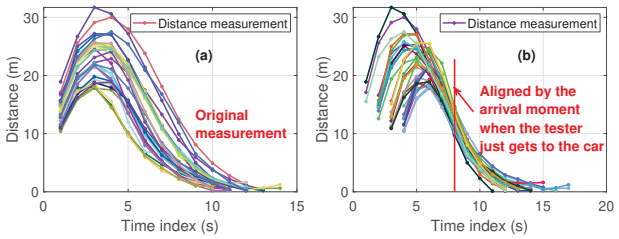

Fig. 5: Distance measurements in which the ISTA moves to the RSTA at a relative high speed (the tester runs to the car).

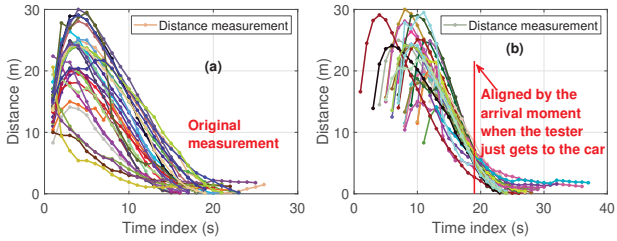

Fig. 6: Distance measurements in which the ISTA moves to the RSTA slowly (the tester walks slowly to the car).

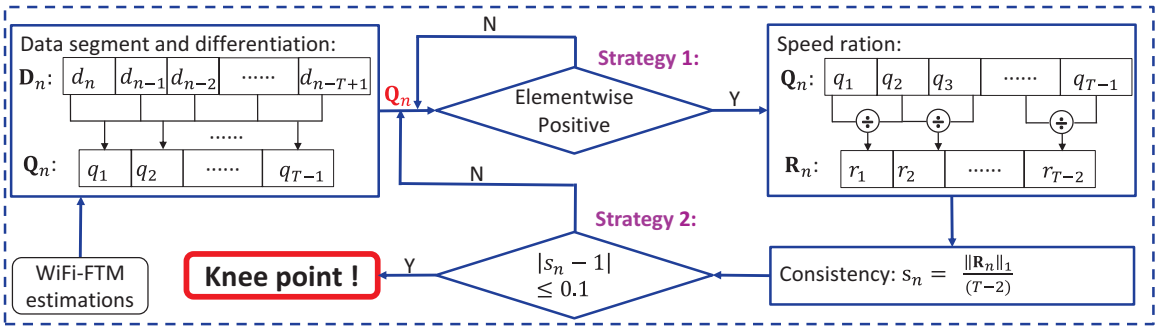

Fig. 7: Key steps of the knee point detection

III. Knee Point and Arrival Time Estimation

A. Knee Point Detection

Assume that we have a WiFi-FTM-based distance sequence $\mathbf{D}_n = [d_n, d_{n-1}, \dots d_2, d_1]$ at time t_n, the instant speed of the ISTA at time t_n can be written as

$$q_n = \frac{d_{n-1} - d_n}{t_n - t_{n-1}}. \tag{2}$$

where t_n and d_n denote the sample time and the WiFi-FTM-based distance estimation at time t_n. To get an averaged/reliable speed estimation, we take the latest T distance points, i.e., $[d_n, d_{n-1}, \cdots, d_{n-T+1}]$, where T is termed as window length as shown in Fig. 7. If the ISTA has stepped into the area where the LOS dominates, $\mathbf{D}_n$ is monotonically decreasing. As a result, every element in the instant speed estimation sequence $Q_n = [q_1, q_2, \cdots, q_{T-1}]$ should be positive (strategy 1 in Fig. 7) since the distance d_n gets smaller and smaller with ISTA approaching the RSTA.

In addition, the natural walking speed of a driver can be assumed as a constant during the whole journey when the driver walks towards his/her car. As a result, the speed estimations within Q_n should be consistent while small deviations are allowed because of the measurement errors. To quantify the speed consistency, we define the average of speed ratios within a window of length T as the speed consistency s_n, which is given by

$$s_n = \frac{||\mathbf{R}_n||_1}{T-2} = \frac{1}{T-2}\sum_{n=1}^{T-2}\frac{q_n}{q_{n+1}}, \tag{3}$$

where $\mathbf{R}_n = [r_1, r_2, \cdots, r_{T-2}]$ represents the speed ratio with $r_i = q_{i+1}/q_i$ $(i = 1, 2, \cdots, T-2)$. Operation $||\cdot||_1$ denotes the l_1-norm. In strategy 2 of Fig. 7, if $|s_n - 1| \leq 0.1$, the speed estimation sequence $\mathbf{Q}_n$ is regarded as a consistent speed estimation sequence and the **knee point** d_n is detected.

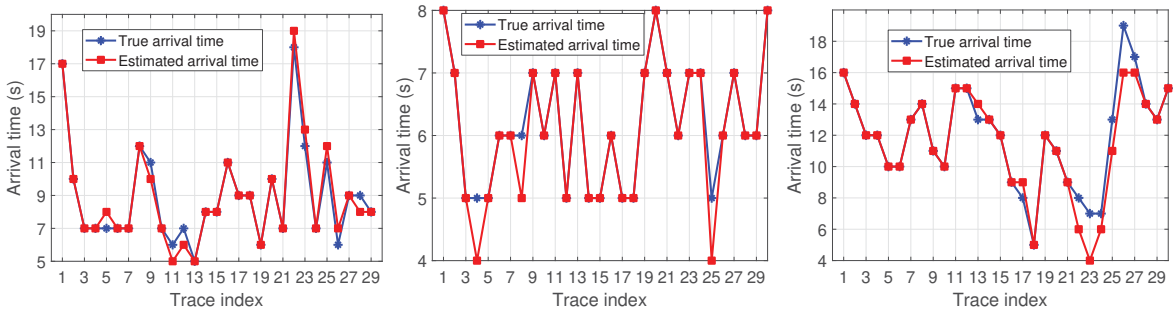

(a) Walking at normal speed (1.2m/s) (b) Normal running (3m/s) (c) Walking very slowly (1m/s)

Fig. 8: Arrival time estimation at different speeds.

TABLE I: Accuracy of the arrival time estimation

#	Parameter/Conditions				Arrival time estimation error: $\hat{\mathrm{T}}^{\mathbf{k}}_{\mathrm{AM}} - \mathrm{T}_{\mathrm{AM}}$					
	Max. initial distance (m)	Same initial distance (Y/N)	Speed	Direction	-3s	-2s	-1s	0s	1s	$\lvert \bullet \rvert \leq 1$s
1	30	N	Normal walking	$0-360°$	6.2%	0	10.4%	83.4%	0	93.8%
2	20	N	Normal running	$0-360°$	0	0	10%	90%	0	100%
3	20	N	Walking slowly	$0-360°$	3.4%	4.1%	10.8%	73.3%	8.4%	92.5%

B. Arrival Time Estimation

To estimate the arrival time, we first define a **LOS-Area** which is centered around the location of RSTA. Within the **LOS-Area**, the LOS signal component dominates and the WiFi-FTM range estimations are accurate. Generally, the **LOS-Area** has different radii in different directions w.r.t. the RSTA due to the impact of multipaths.

To be a knee point, there are two main constraints. First, the knee point should lie on the edge of **LOS-Area**. If the ISTA goes further away than the knee point, the distance estimation accuracy will degrade. Second, once the ISTA passes through the knee point and keeps approaching to the RSTA, the WiFi-FTM distance measurements should be accurate. To meet the two constraints, the knee point should be no further and closer. Assume that the ISTA is $d_{\mathbf{k}}$ away from the RSTA at the knee point and the natural walking speed of a tester is relatively constant, the arrival time can be expressed as

$$\hat{\mathrm{T}}^{\mathbf{k}}_{\mathrm{AM}} = \frac{d_{\mathbf{k}}}{v_{\mathbf{k}}}, \; v_{\mathbf{k}} = \frac{1}{T-1}\sum_{n=1}^{T-1} q_n. \tag{4}$$

Note that the accuracy of the arrival time $\hat{\mathrm{T}}_{\mathrm{AM}}$ can be evaluated based on the recording of the true arrival time T_{AM} once the ISTA arrives at the car.

IV. Performance Evaluation

The experiment set up is the same as described in Section II-B. To evaluate the estimation accuracy of the arrival time T_{AM}, we conduct multiple experiments where a tester walks at different speeds including normal walking at about 1.2m/s, running at about 3m/s and walking very slowly at about 1m/s. For each test, we ask the tester to walk close to the car (RSTA) in 30 different routes and different directions. The initial distance varies from 20m to 30m. Note that we do not need to set all the initial distances as 30m since some specific locations may be occupied by other cars. We repeat the experiment in different parking lots and different testers. The estimated arrival time is shown in Fig. 8, which matches well with the ground truth. More results are given in Table I. Clearly, the proposed method can achieve more than 92% percentile accuracy with no greater than 1s error. From Table I, the estimated arrival time $\hat{\mathrm{T}}^{\mathbf{k}}_{\mathrm{AM}}$ is more likely to be underestimated than the true arrival time T_{AM}. This is because that the WiFi-FTM range measurements correspond to the straight line between the ISTA and RSTA in theory. However, in practice, a tester/ISTA cannot approach to the car/RSTA along the straight line because of obstacles such as other cars. In this sense, the distance measurement is usually shorter than the real walking distance, thus causing underestimation of the arrival time $\hat{\mathrm{T}}^{\mathbf{k}}_{\mathrm{AM}}$.

V. Conclusion

We propose a driver arrival time sensing method by using the WiFi-FTM range estimations which are proved to show a stable changing-trend after a knee point when the ISTA keeps moving close to the RSTA. Based on such observation, we then propose a knee point detection and a driver arrival time estimation scheme. Experimental evaluations using commercial 802.11mc WiFi chipsets show that the proposed system can achieve $\geq 92.5\%$ accuracy with ≤ 1s arrival time estimation error regardless of the environments and users.

REFERENCES

[1] K. J. R. Liu and B. Wang, *Wireless AI: Wireless Sensing, Positioning, IoT, and Communications*, Cambridge University Press, 2019.

[2] B. Wang, Q. Xu, C. Chen, F. Zhang, and K. J. R. Liu, "The promise of radio analytics: A future paradigm of wireless positioning, tracking, and sensing," *IEEE Signal Processing Magazine*, vol. 35, no. 3, pp. 59–80, 2018.

[3] F. Wang, F. Zhang, C. Wu, B. Wang, and K. J. R. Liu, "ViMo: Multi-person vital sign monitoring using commodity millimeter wave radio," *IEEE Internet of Things Journal*, pp. 1–1, 2020.

[4] F. Wang, F. Zhang, C. Wu, B. Wang, and K. J. R. Liu, "Respiration tracking for people counting and recognition," *IEEE Internet of Things Journal*, vol. 7, no. 6, pp. 5233–5245, 2020.

[5] Q. Xu, B. Wang, F. Zhang, D. S. Regani, F. Wang, and K. J. R. Liu, "Wireless ai in smart car: How smart a car can be?," *IEEE Access*, vol. 8, pp. 55091–55112, 2020.

[6] J. L. Wilson, "Automotive wifi availability in dynamic urban canyon environments," *Navigation: Journal of The Institute of Navigation*, vol. 63, no. 2, pp. 161–172, 2016.

[7] F. Wang, J. Liu, and W. Gong, "WiCAR: WiFi-based in-car activity recognition with multi-adversarial domain adaptation," in *2019 IEEE/ACM 27th International Symposium on Quality of Service (IWQoS)*, 2019, pp. 1–10.

[8] S. D. Regani, Q. Xu, B. Wang, M. Wu, and K. J. R. Liu, "Driver authentication for smart car using wireless sensing," *IEEE Internet of Things Journal*, vol. 7, no. 3, pp. 2235–2246, 2020.

[9] L. Li, D. Wen, N. Zheng, and L. Shen, "Cognitive cars: A new frontier for adas research," *IEEE Transactions on Intelligent Transportation Systems*, vol. 13, no. 1, pp. 395–407, 2012.

[10] M. Schreier, V. Willert, and J. Adamy, "Compact representation of dynamic driving environments for adas by parametric free space and dynamic object maps," *IEEE Transactions on Intelligent Transportation Systems*, vol. 17, no. 2, pp. 367–384, 2016.

[11] F. James M, Craig K Allison, Xingda Yan, Roberto Lot, and Neville A Stanton, "Adaptive driver modelling in adas to improve user acceptance: A study using naturalistic data," *Safety Science*, vol. 119, pp. 76–83, 2019.

[12] Wikipedia, "Remote keyless system," [Oline], https://en.wikipedia.org/wiki/Remote_keyless_system, Accessed July 19, 2020.

[13] I. Symeonidis, M. A. Mustafa, and B. Preneel, "Keyless car sharing system: A security and privacy analysis," in *2016 IEEE International Smart Cities Conference (ISC2)*, Sep. 2016, pp. 1–7.

[14] S. Joseph, "Vulnerability in car keyless entry systems allows anyone to open and steal your vehicle," [Oline], https://www.forbes.com/sites/josephsteinberg/2015/05/12/vulnerability-in-car-keyless-entry-systems-allows-anyone-to-open-and-steal-your-car/#199ee87e2442, Accessed May 12, 2015.

[15] L. Matt, "How it works; remote keyless entry: Staying a step ahead of car thieves," [Oline, The New York Times. ISSN 0362-4331], https://www.nytimes.com/2001/06/07/technology/how-it-works-remote-keyless-entry-staying-a-step-ahead-of-car-thieves.html, Accessed February 12, 2017.

[16] M. Ibrahim, H. Liu, M. Jawahar, V. Nguyen, M. Gruteser, R. Howard, B. Yu, and F. Bai, "Verification: Accuracy evaluation of wifi fine time measurements on an open platform," in *Proceedings of the 24th Annual International Conference on Mobile Computing and Networking*, 2018, pp. 417–427.

[17] C. Gentner, M. Ulmschneider, I. Kuehner, and A. Dammann, "WiFi-RTT indoor positioning," in *2020 IEEE/ION Position, Location and Navigation Symposium (PLANS)*, 2020, pp. 1029–1035.

[18] Wikipedia, "Wireless security," [Oline], https://en.wikipedia.org/wiki/Wireless_security, Accessed July 10, 2020.

[19] Google, "Google releases 'wifirttscan app' for testing 802.11mc indoor positioning," [Oline, The New York Times. ISSN 0362-4331], https://9to5google.com/2019/04/14/google-releases-wifirttscan-app/, Accessed April 14, 2019.

[20] L. Banin, O. Bar-Shalom, N. Dvorecki, and Y. Amizur, "Scalable Wi-Fi client self-positioning using cooperative FTM-sensors," *IEEE Transactions on Instrumentation and Measurement*, vol. 68, no. 10, pp. 3686–3698, Oct 2019.